

# Development of a MEMS Acoustic Emission Sensor System

David W. Greve<sup>a</sup>, Irving J. Oppenheim<sup>b\*</sup>, Wei Wu<sup>a</sup>, and Amelia P. Wright<sup>b</sup>

<sup>a</sup>Dept. of Electrical and Computer Engineering, Carnegie Mellon University, Pittsburgh, PA 15213

<sup>b</sup>Dept. of Civil and Environmental Engineering, Carnegie Mellon University, Pittsburgh, PA 15213

## ABSTRACT

An improved multi-channel MEMS chip for acoustic emission sensing has been designed and fabricated in 2006 to create a device that is smaller in size, superior in sensitivity, and more practical to manufacture than earlier designs. The device, fabricated in the MUMPS process, contains four resonant-type capacitive transducers in the frequency range between 100 kHz and 500 kHz on a chip with an area smaller than 2.5 sq. mm. The completed device, with its circuit board, electronics, housing, and connectors, possesses a square footprint measuring 25 mm x 25 mm. The small footprint is an important attribute for an acoustic emission sensor, because multiple sensors must typically be arrayed around a crack location. Superior sensitivity was achieved by a combination of four factors: the reduction of squeeze film damping, a resonant frequency approximating a rigid body mode rather than a bending mode, a ceramic package providing direct acoustic coupling to the structural medium, and high-gain amplifiers implemented on a small circuit board. Manufacture of the system is more practical because of higher yield (lower unit costs) in the MUMPS fabrication task and because of a printed circuit board matching the pin array of the MEMS chip ceramic package for easy assembly and compactness.

The transducers on the MEMS chip incorporate two major mechanical improvements, one involving squeeze film damping and one involving the separation of resonance modes. For equal proportions of hole area to plate area, a triangular layout of etch holes reduces squeeze film damping as compared to the conventional square layout. The effect is modeled analytically, and is verified experimentally by characterization experiments on the new transducers. Structurally, the transducers are plates with spring supports; a rigid plate would be the most sensitive transducer, and bending decreases the sensitivity. In this chip, the structure was designed for an order-of-magnitude separation between the first and the second mode frequency, strongly approximating the desirable rigid plate limit. The effect is modeled analytically and is verified experimentally by measurement of the resonance frequencies in the new transducers. Another improvement arises from the use of a pin grid array ceramic package, in which the MEMS chip is acoustically coupled to the structure with only two interfaces, through a ceramic medium that is negligible in thickness when compared to wavelengths of interest.

Like other acoustic emission sensors, those on the 2006 MEMS chip are sensitive only to displacements normal to the surface on which the device is mounted. To overcome that long-standing limitation, a new MEMS sensor sensitive to in-plane motion has been designed, featuring a different spring-mass mechanism and creating the signal by the change in capacitance between stationary and moving fingers. Predicted damping is much lower for the case of the in-plane sensor, and squeeze-film damping is used selectively to isolate the desired in-plane mechanical response from any unwanted out-of-plane response. The new spring-mass mechanism satisfies the design rules for the PolyMUMPS fabrication (foundry) process. A 3-D MEMS sensor system is presently being fabricated, collocating two in-plane sensors and one out-of-plane sensor at the mm scale, which is very short compared to the acoustic wavelength of interest for stress waves created by acoustic emission events.

**Keywords:** Acoustic emission, MEMS, transducer sensitivity.

---

\* Contact author: [ijo@cmu.edu](mailto:ijo@cmu.edu); 412-268-2950; Carnegie Mellon University, Department of Civil and Environmental Engineering, Pittsburgh, PA, 15213.

## 1. INTRODUCTION

Acoustic emission (AE) testing [1] is used to manage critical civil infrastructure components such as steel bridges and pressure vessels. Those structures have flaws that can approach fracture-critical size with time and use, such as fatigue cracks that grow with repeated loading, and they require periodic inspection. Some fatigue cracks may be stable while others experience continuing growth, and AE sensing is used to distinguish between inactive and active cracks. The term “acoustic emission” refers to transient ultrasonic waves that are released from microscopic zones, such as a crack tip, during irreversible damage, such as crack extension; therefore, acoustic emission events constitute evidence that a crack is active. Conventional AE sensors use piezoceramic elements, whereas in our research we use MEMS fabrication to build capacitive type resonant transducers, with which we create an array of independent transducers on a single small chip. In this paper we describe our design and testing of a 2006 MEMS device collocating four sensors on one chip, less than 5 mm x 5mm in size, with resonant frequencies between 100 kHz and 500 kHz.

Conventional piezoceramic AE sensors, as well as all MEMS AE sensors built to date, are single-axis devices that only detect particle displacements normal to the contact surface. Obtaining time histories of particle displacement in 3-D, referring to the out-of-plane displacement and two orthogonal in-plane displacements, will be a considerable advance in AE sensing. In this paper we also describe the development of a new capacitive-type, resonant transducer that responds to in-plane motion. The resulting MEMS 3-D sensor system will consist of two new in-plane sensors, one responding in the  $x$ -direction and the other in the  $y$ -direction, and one out-of-plane sensor responding in the  $z$ -direction.

## 2. PREVIOUS WORK

Our research team first developed a 2002 MEMS device [2] for AE sensing featuring a suite of 18 capacitive-type resonant sensors at ten different frequencies. Two different vibration mechanisms were employed: hexagonal plates in bending to create the high-frequency sensors, and spring-mass systems formed by plates supported by L-shaped bending springs to create the low-frequency sensors. The device, 10-mm square, was fabricated in the MUMPS three-layer polysilicon surface micromachining process; stationary capacitor plates were fabricated in the lowest Poly0 layer, and the vibrating structures (the hexagonal bending plates, or the “piston” plates in the spring-mass systems) were fabricated in the next Poly1 layer. Squeeze-film damping was high, because of the small gap (1.25  $\mu\text{m}$ ) between the vibrating plate and the stationary plate forming the capacitor, and therefore the resonances were observable only under a vacuum environment. Laboratory studies showed that the MEMS sensors, under vacuum, could detect stress waves in steel specimens when acoustic emission was simulated physically by pencil lead breaks or ball impacts, and that the information extracted from the transducer signals could be used for source localization.

Based upon those experimental findings, a 2004 MEMS device was developed [3] to operate under atmospheric pressure. This 2004 MEMS device featured six transducers with design resonant frequencies between 101 and 506 kHz, and a seventh transducer at 1 MHz, occupying a 10-mm square die. Compared to the first device, the area of each individual transducer was enlarged in order to increase the capacitance and thereby the transducer sensitivity, and the etch hole spacing was significantly decreased in order to reduce the squeeze-film damping and thereby achieve a moderately underdamped response. This second MEMS device was used successfully in laboratory testing and demonstrated in a field test [4].

Careful examination of the vibration characteristics of the spring-plate mechanism in the second MEMS device [5] revealed two mechanical conditions that were limiting the performance of the sensors. Those two conditions are reviewed here:

- Because of bending deformation in the plate, a second mode response was observed that coupled strongly to the desired first mode response. (Throughout this paper, when referring to first and second modes, we restrict ourselves to *active* modes that respond mechanically to the out-of-plane excitation and that respond electrically with a first-order change in capacitance. Numerous other modes exist that do not demonstrate first-order response and therefore may be considered inactive by comparison.) We take as our discussion example a sensor with a predicted resonant frequency of 266 kHz as a pure spring-mass system, which would be a pure translation of the plate. That particular sensor exhibits one experimental resonance at 187 kHz and a second at 266 kHz. FEM simulations indicate that the first resonance corresponds to a mode consisting mostly of

translation but considerably softened by bending, whereas the second resonance consists mostly of plate bending but softened by translation [5]. Because stress waves generated in acoustic emission events are most energetic in the frequency range between 100 kHz and 500 kHz, both modes would be excited in an AE event, leading to complications in the interpretation the resulting signal would be expected. It was recognized that superior performance would be obtained if response in the first mode was dominant, a principle which was followed in the design of the 2006 MEMS device reported here.

- Although squeeze-film damping was greatly reduced, and the sensor response was sufficient to operate under atmospheric conditions, the Q factor was modest. For example, for the aforementioned sensor with a predicted resonant frequency of 266 kHz the measured Q factor was only 1.7 [5], whereas a higher Q factor (less damping) would be desirable. Therefore, additional efforts to reduce squeeze-film damping were undertaken in the development of the present structure.

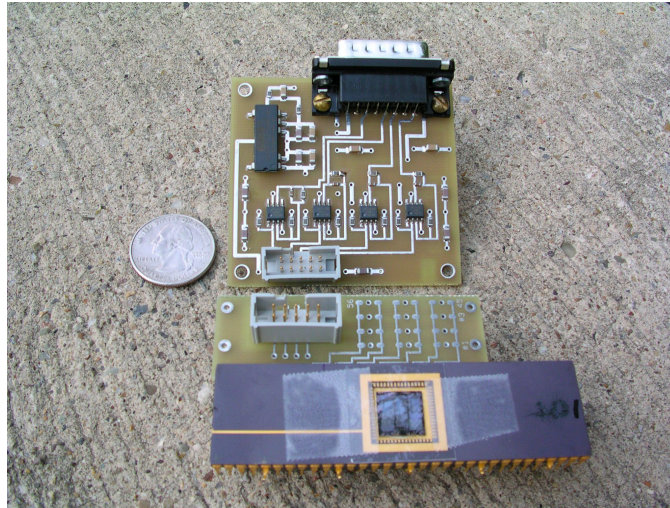


Figure 1. 2004 MEMS device and custom PC board with 4-channel amplification; housing (not shown) 45x50x90 mm

Other aspects that have been addressed in the design of the 2006 MEMS device include acoustic coupling to the structural medium and reduction of the sensor contact footprint. Figure 1 shows the 2004 MEMS device mounted in a ceramic DIP package [4], to the underside of which a steel bar (15-mm square) was affixed with epoxy to provide coupling to the steel structure. Figure 1 also shows the custom PC board containing four channels of amplification. When assembled within its housing the resulting 4-channel AE sensor system occupies a 50 mm x 90 mm footprint, which compares favorably to single-channel commercial devices with their magnetic hold-downs, but is larger than necessary. The housing size for the 2004 MEMS device was governed by the size of the available ceramic package, and reducing that size was another factor addressed in the 2006 device.

### 3. DESCRIPTION OF 2006 MEMS DEVICE

Fabrication of the improved MEMS device features subdicing each 10-mm square die into four subchips, so that each device is less than 5 mm square and the batch yield is quadrupled to 60 rather than 15. Each device contains four sensors with resonant frequencies in the range from 100 kHz to 500 kHz, and we presently mount the chip in a ceramic package 25 mm square.

Figure 2 shows the CAD layout of a single die, subdiced to create four 5-mm square subchips. Each device (each 5-mm square subchip) contains four independent sensors. Figure 3 shows the CAD layout of a typical sensor, consisting of 144 spring-plate units in parallel; each plate in the 2006 MEMS device is 125  $\mu\text{m}$  square, as contrasted to dimensions ranging from 270 to 380  $\mu\text{m}$  in the 2004 device. The smaller plate size limits the influence of plate bending on the vibration behavior. Moreover, the etch holes have been placed on a triangular layout rather than a square layout. The effect of this change in etch hole geometry, for an equal ratio of etch hole area to plate area, is to reduce the maximum distance

traveled by air forced through the etch hole by out-of-plane motion. The squeeze-film damping effect would thereby be reduced, and a higher Q should be achieved.

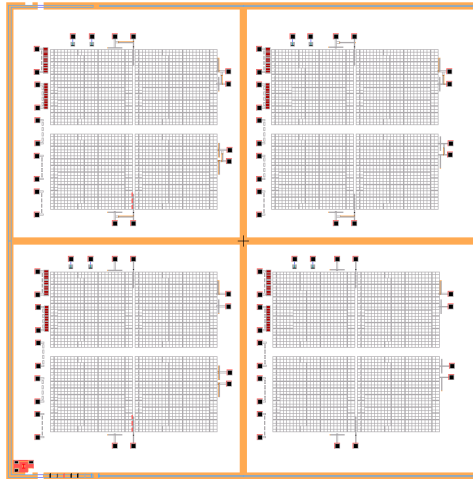


Figure 2. CAD layout of four 2006 MEMS devices

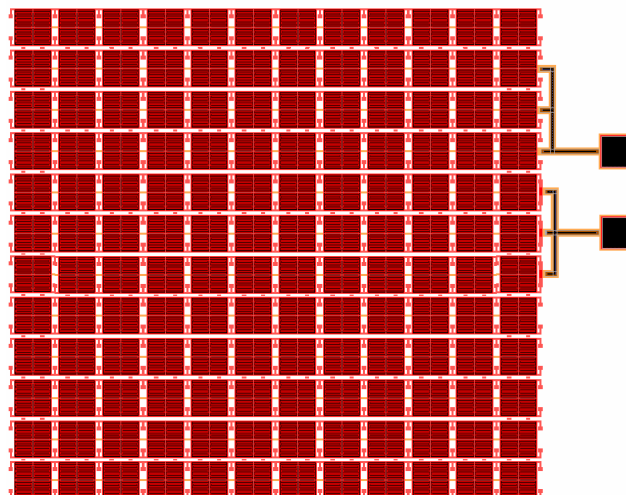


Figure 3. CAD layout of typical single sensor, consisting of 144 spring-plate units in parallel.

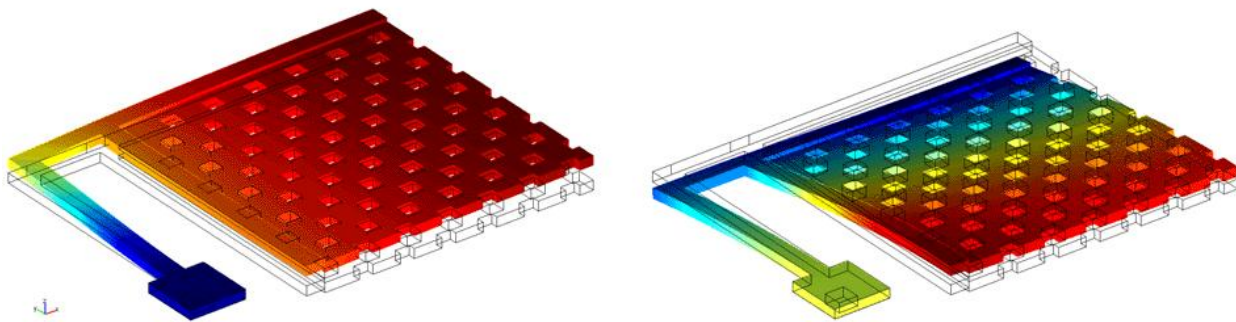


Figure 4. FEM simulation of quarter-plate, with lowest two eigenmodes of interest at 180 kHz (left) and 1.02 MHz (right).

FEM simulation studies were used to approach the ideal response of pure translation in the first mode, well separated in frequency from the second mode. Figure 4 shows pertinent FEM results for the quarter-plate, 60  $\mu\text{m}$  square. The mode shape at the fundamental frequency of 180 kHz is an almost pure translation of the plate with minimal bending deformation, and the frequency of the next active mode is 1.02 MHz, which is well separated from the operating frequency of 180 kHz.



Figure 5. (a) 2006 MEMS device mounted in pin grid array package; (b) 2006 MEMS sensor system, with electronics, on steel plate.

The 2006 MEMS device has been mounted in a ceramic pin grid array package, only 25-mm square, which is shown in Figure 5a during characterization measurements. The package geometry features a flat bottom, which is well-suited for acoustic coupling to a structural substrate, and the pin geometry permits direct electrical connection to a custom PC board containing the four amplifier circuits. A resulting sensor system exploiting both of those advantages is shown in Figure 5b, where the system is mounted on a steel plate with its housing/shielding removed. The four-channel system is contained in a 25 mm x 25 mm x 15 mm volume.

#### 4. CHARACTERIZATION MEASUREMENTS

Figure 6 shows a representative C-V measurement, for a device with a predicted resonant frequency of 404 kHz, showing a capacitance of 14.36 pF in the undeflected state. There is a design tradeoff between the overall device size and the capacitance of an individual sensor, and in the 2006 MEMS device the sensor capacitance has been reduced compared to the 2004 design, to a target capacitance of 13 pF. C-V measurements were performed on seven different sensors, and the undeflected capacitance was observed to range from 11.96 to 17.53 pF.

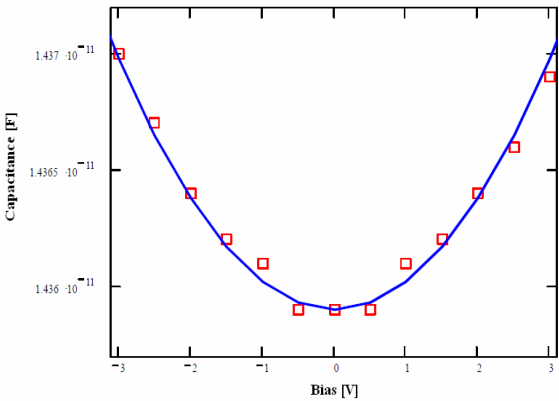


Figure 6. C-V measurement, 404 kHz sensor

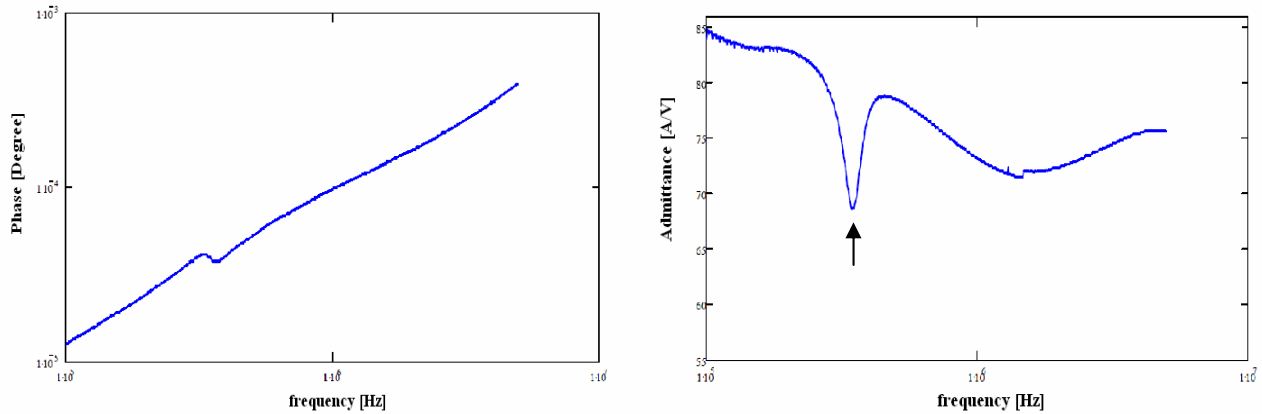


Figure 7. Admittance measurements for 404 kHz sensor, showing resonance at 345 kHz

Figure 7 shows admittance measurements from which the resonant frequency and damping of a sensor are extracted. In this instance, the sharp minimum corresponds to a resonant frequency of 345 kHz, as compared to the predicted frequency of 404 kHz for this sensor. Most significantly, no second resonance is observed below 1 MHz. The Q factor is extracted by fitting appropriate coefficients into an equation for dynamic response [6] and matching the experimental plot, as shown in Figure 8. In this case, a Q factor of 5.39 was extracted for the sensor, which is significantly higher than typical Q factors for the 2004 MEMS device [5].

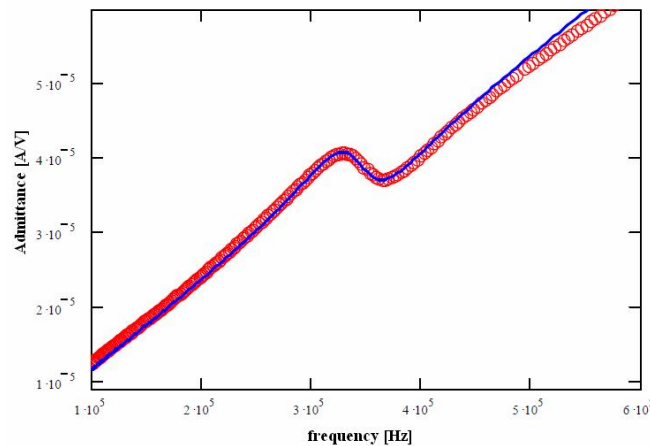


Figure 8. Fit to admittance measurement, used to extract Q factor of 5.39

A custom PC board interconnects to the pin grid array, as shown in Figure 5b. The board contains four independent amplifiers with a nominal gain of 100; a representative test of one amplifier yielded a measured voltage gain of 98.7. The amplifier shown in Figure 5b does not show the external battery pack. In our subsequent tests we have used two levels of bias voltage, 9 V for the two lower frequency sensors on the chip, and 18 V for the two higher frequency sensors on the chip. The bias voltage must be set safely below the pull-down collapse voltage, and the lower frequency sensors, with softer springs, have lower collapse voltages.

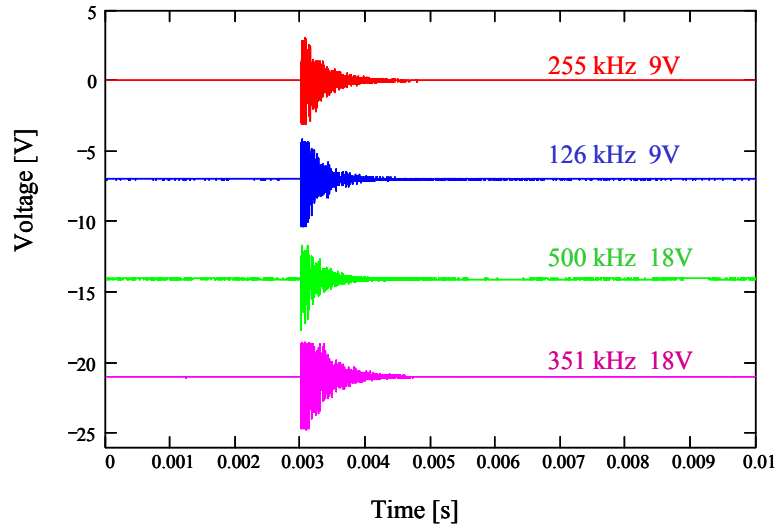


Figure 9. Sensor system response to pencil-lead break applied to ceramic package

Figure 9 shows the response of the four sensors to a pencil-lead break applied to the ceramic package. (The four subchips shown in Figure 2 are not identical, because other AE research activities dictated the design of somewhat different subchips. Therefore, the subchip tested in Figure 9 is different from the one tested in Figures 7 and 8, which is why a sensor with a nominal resonant frequency of 404 kHz does not appear in Figure 9.) Tests of the system on steel plates and in field applications are underway.

## 5. IN-PLANE DEVICE FOR 3-D MEMS AE SENSING SYSTEM

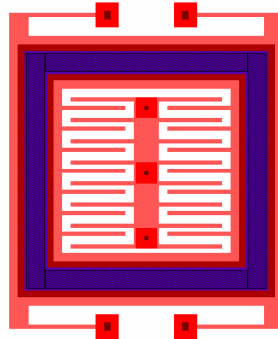


Figure 10. CAD layout of spring-mass unit for in-plane (y-direction) response

Figure 10 shows, to scale, the CAD layout of a sensor unit designed to respond to in-plane excitation, satisfying the design rules of the PolyMUMPS process. It contains a stationary central spine with projecting stationary fingers, which form capacitors with moving fingers that project from a spring-mounted frame. Features of the design are outlined as follows:

- The frame shown in Figure 10 is approximately  $130\ \mu\text{m}$  square. The unit shown has a predicted resonant frequency of 250 kHz, and changing the length of the L-shaped springs makes it possible to design the units for resonant frequencies in the range from 100 to 500 KHz.
- The pitch (spacing) between fingers is unsymmetrical, in order to effect a change in capacitance during motion.
- Each sensor consists of a number of units acting in parallel. Design calculations establish that suitable sensitivity will be achieved with a number of units that pack effectively at the mm-scale, easily permitting the fabrication of three independent sensors on the die site.

- A quality factor  $Q$  in excess of 1000 is predicted for the in-plane response of the sensor unit shown in Figure 10, which is higher by two orders of magnitude than the quality factors typically obtained with our sensor units designed for out-of-plane response. The in-plane  $Q$  is comparatively high because viscous damping produced by air in the gap beneath the spring-mounted frame corresponds to the kinematics of one plate translating parallel to another, rather than to squeeze-film flow, and because radiation (into air) is minimal in the in-plane direction of motion.
- Additional dissipative mechanisms are of course present, and therefore the in-plane  $Q$  will be less than predicted above. Nonetheless, the  $Q$  may still be higher than ideal for the intended application, with the potential to produce undesirable ringing. Additional damping will be supplied electrically, giving the designer control over the resulting sensor damping.
- The spring-mounted frame shown in Figure 10 will have a mechanical resonance in the out-of-plane direction (the  $z$ -direction) as well. It is necessary to isolate  $y$ -direction response from  $z$ -direction response, and an elegant solution has been identified. High damping in the  $z$ -direction is easily created by squeeze film damping. Colloquially, the frame will move with little damping in the  $y$ -direction while it “floats on a bed of air” that precludes significant movement in the  $z$ -direction. The mechanical configuration of the unit provides the designer with several variables (such as frame width and etch hole spacing) that can be chosen to achieve a target squeeze-film damping and achieve a target isolation of  $y$ -direction from  $z$ -direction motion.
- The 3-D MEMS AE sensor system will consist of two in-plane sensors and one out-of-plane sensor, collocated at a scale which is much shorter than the wavelengths associated with stress waves of interest in AE testing.
- The  $z$ -direction sensor (not shown) will also exploit a finger design, but the aforementioned variables of frame width and etch hole spacing will be chosen to minimize squeeze-film damping and radiation damping. There is considerable latitude in the frame width and etch hole spacing dimensions, and the designer can create structures (satisfying the design rules) that range from high squeeze-film damping, as needed for the in-plane sensor, to low squeeze-film damping, as needed for the out-of-plane sensor. Our calculations suggest that a significant improvement in the sensitivity of the  $z$ -direction sensor, as compared to our 2006 MEMS device, can be achieved using the finger design.

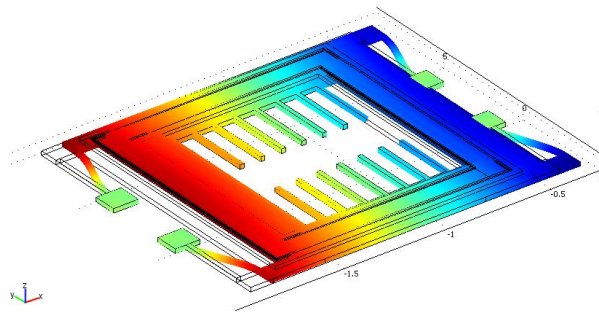


Figure 11. In-plane vibration mode of frame unit

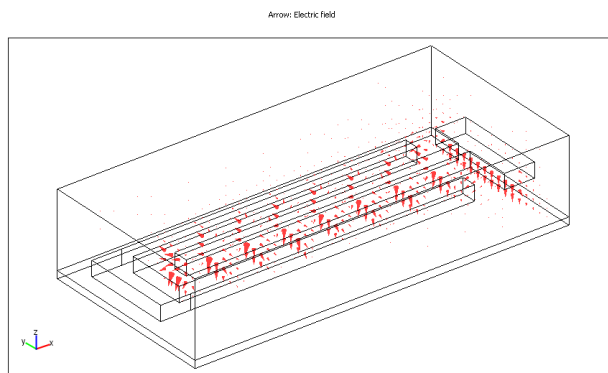


Figure 12. Simulation of 3-D electric field between moving and stationary fingers

Figures 11 and 12 show FEM simulations that have been used in the design of the in-plane sensing unit. The vibration simulation shown in Figure 11 confirms the resonant frequency and mode shape for the intended response. It shows a desired near-perfect translation condition, and related images (not shown) show that unwanted out-of-plane components and that bending effects (other than the intended bending in the springs) are negligible. Simulation results for other modes, not shown, establish that the next mode that is active both electrically and mechanically occurs at a frequency well in excess of 1 MHz, and is therefore well separated from the mode of interest. Figure 12 depicts results of an FEM electrostatic simulation of charge on surfaces of a moving finger and its neighboring stationary fingers; the simulation models the positive contribution of fringe capacitance, obtained from the full 3-D solution for the electric field as contrasted to a parallel-plate model. The 3-D MEMS AE sensor is currently being fabricated.

## 6. DISCUSSION AND CONCLUSIONS

The 2006 MEMS AE device reported here features four resonant sensors, with frequencies between 100 kHz and 500 kHz, on a chip that is 5 mm square. A typical sensor on the device demonstrates a first mode response that is relatively close to the ideal of a spring-plate system in pure translation, with a frequency that is well separated from that of the second mode. A typical sensor on the device exhibits higher Q than sensors on the 2004 device, partly because of a change from a square layout to a triangular layout of etch holes. Each MEMS device occupies only one-quarter of a die site, so that the yield from a regular batch in the PolyMUMPS process is 60 devices rather than 15. The new device is mounted in a pin grid array ceramic package with a geometry permitting superior acoustic coupling to a structural substrate and a more compact four-channel system, with a 25 mm x 25 mm footprint. A related MEMS sensor design is sensitive to in-plane motion, featuring a spring-mass mechanism vibrating in the plane of the MEMS device, and creating the signal by the change in capacitance between stationary and moving fingers. A 3-D MEMS sensor system is presently being fabricated, collocating two in-plane sensors and one out-of-plane sensor at the mm scale.

## ACKNOWLEDGEMENTS

This material is based upon work supported by the National Science Foundation under Grant No. CMS-0329880 entitled *SENSORS: Collaborative Research: MEMS for Multi-Mode Civil Infrastructure Sensing*, by the Pennsylvania Infrastructure Technology Alliance, by Carnegie Mellon University, and by Lehigh University. We are indebted to our research collaborators at Lehigh University, Professor S. P. Pessiki and Dr. D. Ozevin, who is now a Research Scientist with Physical Acoustics Corporation. The opinions, findings, conclusions, and recommendations expressed in this material are those of the authors and do not necessarily reflect the views of the sponsors.

## REFERENCES

1. Hellier, C. J., *Handbook of Nondestructive Evaluation*, McGraw-Hill, 2002.
2. Ozevin, D. Greve, D. W., Oppenheim, I. J., and Pessiki, S. P., "Steel Plate Coupled Behavior of MEMS Transducer Developed for Acoustic Emission Testing," *26th European Conference on Acoustic Emission Testing (EWGAE)*, Berlin, September 2004.
3. Ozevin, D., Greve, D. W., Oppenheim, I. J., and Pessiki, S. P., "Design, Characterization and Experimental Use of an Optimized MEMS Acoustic Emission Device," *SPIE Smart Structures/NDE Joint Conference*, 2005, Paper 5765-48.
4. Oppenheim, I. J., D. W. Greve, D. R. Hay, Y. R. Hay, D. Ozevin, S. P. Pessiki, and N. L. Tyson, "Structural Tests Using a MEMS Acoustic Emission Transducer," *SPIE Smart Structures/NDE Joint Conference*, 2006, Paper 6174-02.
5. Ozevin, D., D. W. Greve, I. J. Oppenheim, I. J., and S. P. Pessiki, "Resonant capacitive MEMS acoustic emission transducers," *Smart Mater. Struct.* 15 (2006) pp. 1863-1871.
6. Oppenheim, I., A. Jain, and D. Greve, "Electrical characterization of coupled and uncoupled MEMS ultrasonic transducers," *IEEE Transactions on Ultrasonics, Ferroelectrics, and Frequency Control*, 2003, pp. 297-304.